Comparative Medicine
Copyright 2002
by the American Association for Laboratory Animal Science

Vol 52, No 5
October 2002
Pages 433-438

Magnetic Resonance Imaging Assessment of a Murine Model of Recessive Polycystic Kidney Disease

Yanping Sun, PhD,[1,*] Jing Zhou, PhD,[2] Cherie Stayner, PhD,[2] Jeeva Munasinghe, PhD,[4] Xiaohua Shen, MD,[2] David R. Beier, PhD,[3] and Mitchell S. Albert, PhD[1]

Purpose: **The pathogenesis of polycystic kidney disease (PKD) has not been firmly established; however, our current knowledge of cystogenesis and human cystic disease has been greatly advanced by a variety of animal models of PKD. To study the onset and degree of cyst formation in PKD mouse models without requiring sacrifice of these animals, we have initiated magnetic resonance imaging (MRI) studies of the juvenile cystic kidney (jck) mouse model.**

Methods: **The MRI experiments were performed by use of a Bruker 8.5 T system, on seven-week-old mice that were homozygous for the recessive *jck* mutation and that manifested PKD. Kidney volume was measured, using three-dimensional segmentation postprocessing techniques.**

Results: **The MR images of the enlarged kidneys from affected mice had regions of high signal intensity, with a radial distribution, which reflected the dilated collecting ducts observed in the corresponding histologic slices. The volume of PKD-affected kidney was about 4 times greater than that of the normal kidney.**

Conclusions: **Magnetic resonance imaging has the ability to non-invasively assess cystic disease in mouse models of PKD. Of considerable importance is the opportunity to characterize this disease without sacrificing the animal. The three-dimensional MRI segmentation method provides accurate calculation of renal volume.**

Determination of the mammalian genome sequence is progressing rapidly; the challenge for the future will be the functional characterization of gene products. Of particular interest are the proteins involved in human disease, and for this purpose, analysis of mouse models is likely to have a substantial role. The well-characterized genetics of the mouse, existence of inbred strains, ability to manipulate the genome using transgenesis, and highly efficient methods of mutagenesis provide powerful and complementary tools for functional analysis. Given the importance of mouse methods for biomedical studies, the reliance on necropsy and histologic analysis for pathologic characterization represents a significant limitation. Development of models for non-invasive imaging will have usefulness for a wide variety of investigations. We describe how magnetic resonance imaging (MRI) can be used to analyze recessive polycystic kidney disease (PKD) in a mouse model.

The juvenile cystic kidneys (*jck*) mutation currently under investigation arose in a transgenic line of homozygous mice having a presumptive insertional mutation that results in perinatal death (1). Although the *jck* mutation occurred in this transgenic line, it is not directly attributable to the transgene, since the mutation segregates freely from it and has been crossed out of the stock used to maintain the *jck* mutation. Mendelian genetic analysis established *jck* as a recessive mutation, not allelic with other known mutations predisposing to PKD (2). The course of polycystic disease in jck mice is consistent in the C57BL/6J background in which it was found. Enlarged kidneys cannot usually be palpated prior to four to five weeks of age, but are detected in affected mice by seven weeks. Mice generally survive at least 20, but not longer than 25 weeks.

The study of PKD by use of imaging techniques is an area in which experience in human disease presently exceeds that investigated by use of animal models. Ultrasound has emerged as an important imaging tool that establishes the diagnosis and progression of PKD. This technique, however, has limited sensitivity in young patients with an early stage of disease. Diagnosis of PKD is typically confirmed, using computed tomography, but use of the required intravenous contrast material is often contraindicated in the presence of renal failure. The motivations for using MRI in the kidney arise from clinical applications and basic science interest (3-7). Magnetic resonance imaging represents a continuing revolution in medical technology, providing detailed images of the human body with unprecedented soft tissue contrast. Due to the innate versatility of this modality, tissue anatomy, pathology, metabolism, and perfusion are all amenable to noninvasive evaluation. Moreover, the MR signal dependence is ideal for qualitative and quantitative analysis.

We describe the application of MRI to study juvenile cystic kidneys, using our jck mouse model. Preliminary findings indicate that complex renal lesions seen on MR images correlate with histopathologic findings. Using three-dimensional (3-D) segmentation postprocessing techniques to extract further information from the 2-D MR images, volume of the kidneys was measured. In addition, the volume was assessed using the for-

Received: 4/08/02. Revision requested: 5/08/02. Accepted: 6/26/02.
[1]Department of Radiology, [2]Renal Division, Department of Medicine, [3]Genetics Division, Department of Medicine, Brigham and Women's Hospital, 221 Longwood Avenue, Boston, Massachusetts 02115, and [4]Department of Radiology, Beth Israel Deaconess Medical Center, Boston, Massachusetts.
[*]Corresponding author.

mula for an ellipsoid, and a comparison between the two methods is described.

Methods

Mouse model. Seven-week-old male C57BL/6J mice were used, as the strain in which the PKD mutation was maintained (n = 1), and as the strain used for the control mice (n = 1). They were fed a regular diet of Purina Lab Chow and water ad libitum, in an air-conditional animal room at 22 ± 3°C, with relative humidity of 55 ± 5%. The Harvard Medical Area Standing Committee on Animals reviewed and approved all experimental procedures and housing conditions. The experimental mouse was homozygous for the recessive mutation juvenile cystic kidney (*jck*), and had enlarged and readily palpable kidneys. The *jck* mutation arose spontaneously in the mouse (2) and has been mapped to chromosome 11 (8).

Magnetic resonance imaging acquisition. The MRI experiments were performed, using a Bruker 8.45 T bore system (Bruker Instruments, Inc., Billerica, Mass.). Mice were anesthetized by intraperitoneal injection of 3.6% chloral hydrate (0.01 ml/g of body weight). A rigid bite-bar on a home-built nonmagnetic animal holder was used to hold the anesthetized mouse in vertical position, with the rostral end up, within a saddle-shaped Helmholtz coil, 2.56 cm in diameter. Multi-slice coronal and axial images were acquired, using a standard spin-echo sequence with a repetition time (TR) of 1,500 milliseconds and an echo time (TE) of 25 milliseconds. Coronal images were produced by use of a 128 × 128 matrix, one signal average, and a 3.60-cm field of view (FOV) for normal kidneys, and a 5.00-cm FOV for PKD-affected kidneys. Axial images were acquired, using a 2.56-cm FOV, 256 × 256 matrix, and four signal averages. In both instances, slice thickness was 1 mm.

Imaging processing and volume calculation. After the MR scans were obtained, an interactive distance measurement was performed, using image visualization and analysis tools (ParaVision software package developed by Bruker Instruments). Kidney volume was calculated, using the ellipsoid formula (Volume = length * width * thickness * π/6) (9). Maximal length of the kidney was measured in the coronal plane; width and thickness were measured in the transverse plane and at the hilum. Width was also measured at the largest transverse diameter. For both width measurements, separate volumes were calculated and named Vh (hilum) and Vm (maximum), as appropriate.

The MR imaging data was transferred to a Sun-Workstation (Ultra 60, Sun Microsystems Inc., Mountain View, Calif.). Coronal images were segmented, using 3-D slicer software developed in the Surgical Planning Laboratory at our institution. Segmentation consists of outlining shapes on 2-D gray-scale images and assigning each voxel to the appropriate organ. To identify the kidneys, we applied automatic segmentation algorithms based on the different threshold values for different organs. To separate the boundaries of the kidney from the surrounding tissue (in instances where they had the same signal intensity), we manually edited the organ by use of a segmentation line, thus identifying landmarks for the virtual kidney. Using the segmented labels, we generated 3-D models. Using MRX software, another suite of tools developed in the Surgical Planning Laboratory, we tallied the total number of voxels lying within the boundaries of the kidney and multiplied by the voxel size to yield the volume.

Calibration of MRI volume measurement was achieved by measuring the volume of a series of phantoms containing 1 m*M* gadopentetate dimeglumine (Berlex Laboratories, Wayne, N.J.) in saline, using the same MRI acquisition protocol used for scanning the mice. The 'actual volumes' of the phantoms, calibrated using a volumetric pipette, were 0.05, 0.20, 0.60, 1.0, 2.0 and 2.6 ml. Phantom volumes were quantified from MRI data sets, using 3-D slicer and MRX software and were compared with the actual volume of each phantom to determine the accuracy of the MRI segmentation method. The kidney volume estimates generated using the formula for an ellipsoid were compared with those derived from the 3-D segmentation technique.

Histologic slide preparation. Mice with and without PKD were sacrificed after the MRI experiments were completed; their kidneys were harvested and fixed in formalin. The fixed kidneys were later embedded in paraffin and sectioned at 4-μm thickness, and were stained with hematoxylin and eosin. Photographs were taken, using a dissecting microscope (Leica, M26, Burlington, Mass.), including an entire cross section of the kidneys.

Results

Histologic analysis. Cross sections of mouse kidneys with and without PKD are seen in Fig. 1 (a and b). The kidneys from mice with PKD were significantly larger than those from clinically normal age-matched controls, with extensive cystic lesions replacing normal renal parenchyma. These cysts, lined by flattened epithelium, were observed in the cortical and medullary regions of the PKD-affected kidney. This is consistent with the previously reported characterization of the jck PKD mouse phenotype (2) in which renal cystic changes progressively developed, and by seven weeks of age, were seen to affect almost the entire kidney.

Results of MRI. Animals tolerated the imaging procedure well without adverse effects from either the environment within the magnet or from the anesthesia. Axial and coronal proton density (TR = 1,500 milliseconds, TE = 25 milliseconds) spin-echo images of the PKD mouse and wild-type mouse are shown in Fig. 2 and 3. Compared with those of the wild-type mouse, there is a striking enlargement of the kidneys in the PKD mouse as well as distention of the abdominal cavity. The PKD-affected kidneys maintained their reniform shape, but appeared hyperintense, compared with the wild-type tissue. We also observed rows of elongated structures in the kidneys of the PKD mouse, most notably in the cortex, that matched the corresponding pattern of dilated, cystic lesions observed in histologic sections. In addition, the radial distribution of dilated structures had replaced the normal corticomedullary junction. This pattern was apparent in all slices of both diseased kidneys.

Three-dimensional rendering of the segmented images in Fig. 4 (a and b) show size of the kidneys. The 3-D views add additional information than would otherwise be obtained from conventional MRI alone.

Accuracy of 3-D MRI segmentation for volume measurements. To determine the accuracy of the 3-D MRI volume quantification technique, we prepared a series of phantoms containing various known volumes of saline, as described in the Methods section. Figure 5 shows the "actual" phantom volumes plotted against volumes determined by MRI. Close agreement between MRI and actual phantom volumes suggests that the 3-D MRI segmentation method is accurate.

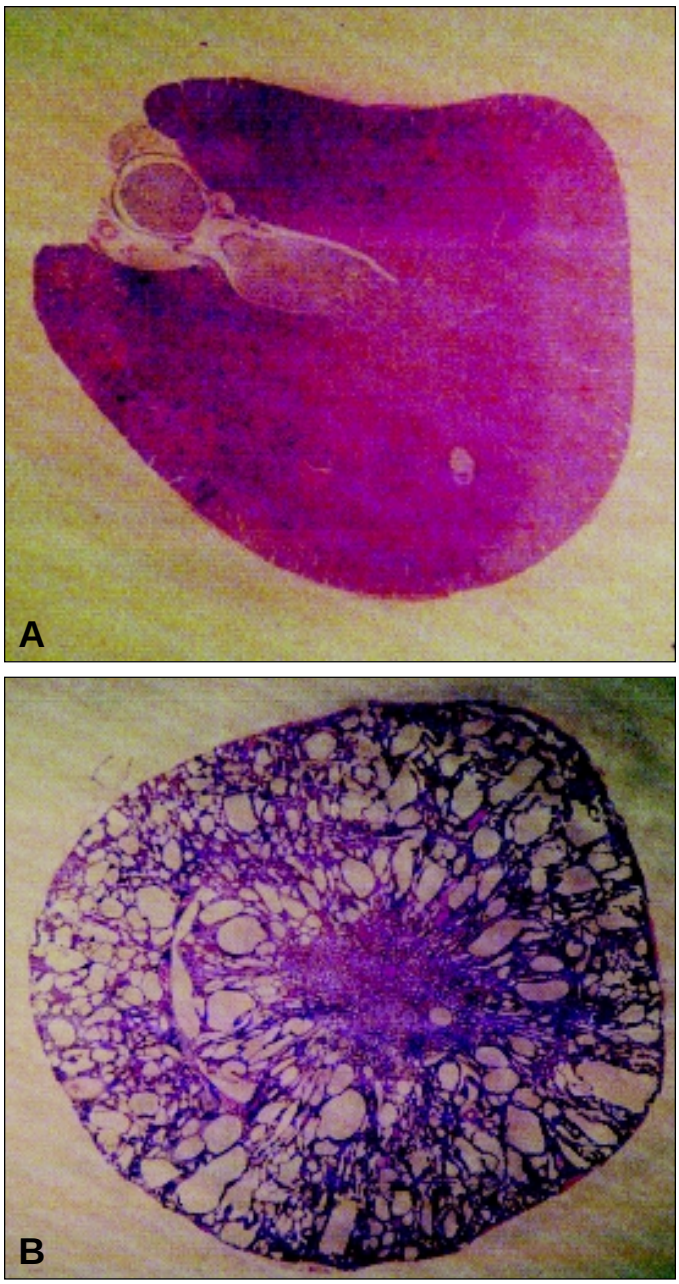

Figure 1. Photomicrographs of a section of (A) wild-type mouse kidney and (B) kidney from a mouse with polycystic kidney disease (PKD). The kidneys were sectioned at 4-µm thickness, and were stained with H&E. Images on a dissecting microscope were taken at 10× magnification.

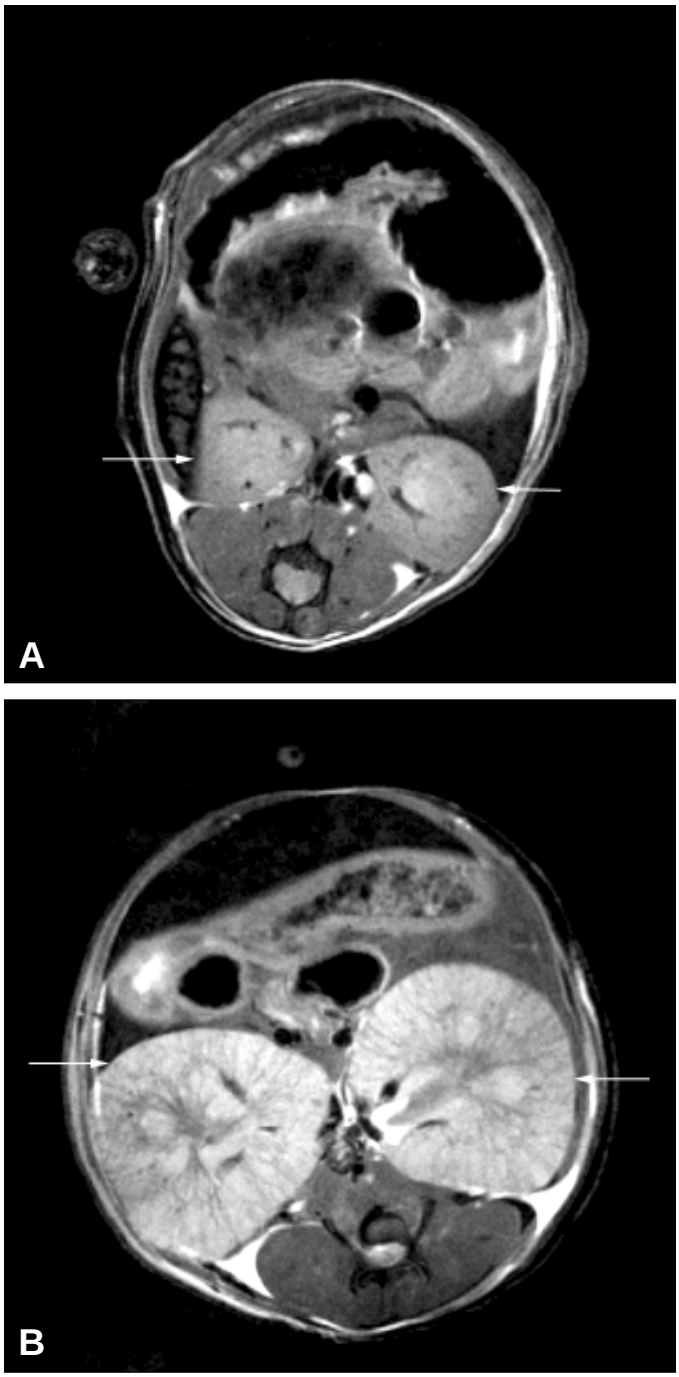

Figure 2. Two-dimensional axial MR images of (A) wild-type mouse kidney and (B) PKD-affected kidney. Arrows indicate location of the kidneys.

Kidney volume calculations. The kidney volume calculations are shown in Table 1. Use of the ellipsoid formula for volume calculations on 2-D MRI slices gave an underestimation of the volume, compared with use of the 3-D segmentation method. The kidney volume was underestimated by an average of 22% when the width was determined at the hilum. Although a second measurement taken at the maximal transverse diameter of the kidney gave a volume closer to that obtained using the 3-D MRI technique, it still underestimated the volume by an average of 12%.

Discussion

Polycystic kidney disease is a genetically heterogeneous group of disorders that represent the fourth most common cause of end-stage renal failure. Despite recent progress in elucidating the function of proteins known to be mutated in human autosomal-dominant polycystic kidney disease (ADPKD), the exact role of the polycystin genes in maintaining renal tubular integrity is still not clear. In this regard, investigation of spontaneous and targeted animal models of PKD is essential to understanding the cause and process of the disease.

In many respects, the abnormalities in jck mutant mice are similar to those found in human polycystic kidney disease. With

Figure 3. Two-dimensional coronal MR images of (A) wild-type mouse kidney and (B) PKD-affected kidney. Arrows indicate location of the kidneys.

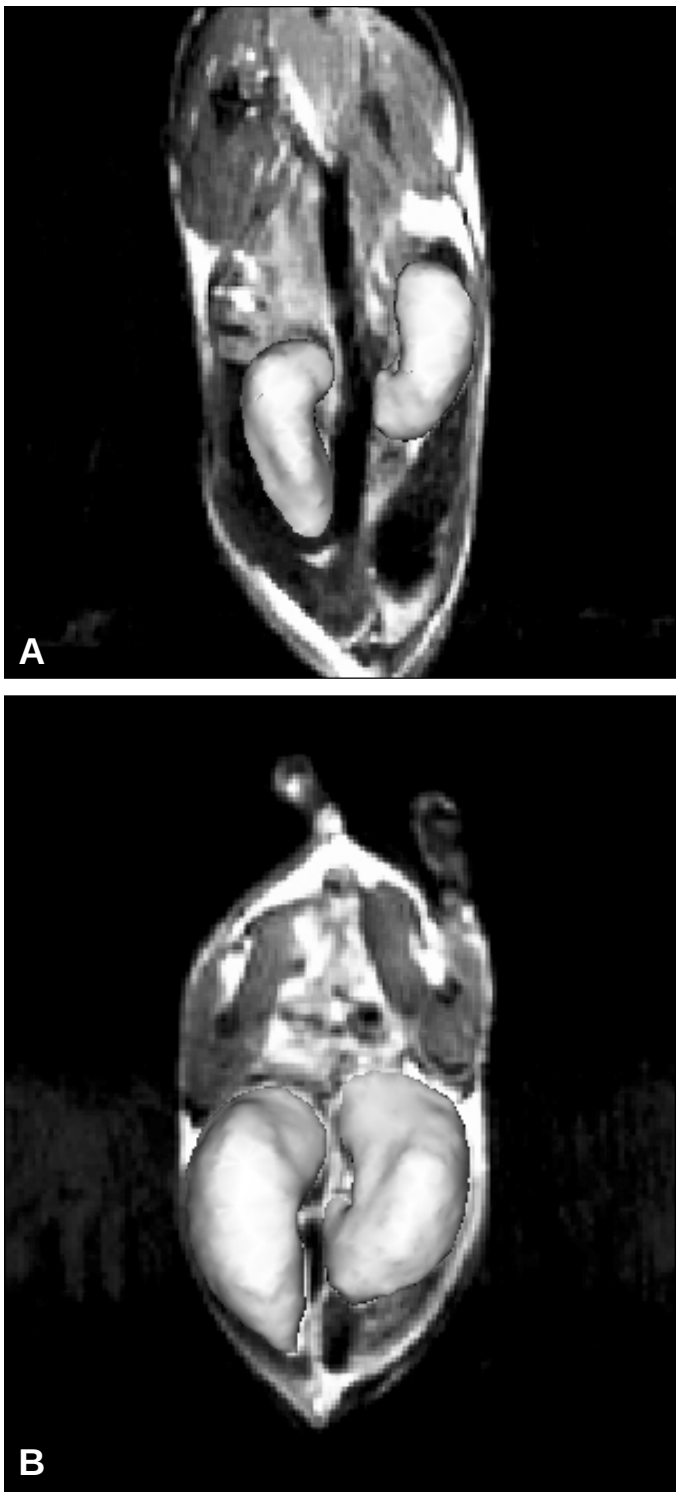

Figure 4. Three-dimensional MRI renderings of the segmented (A) wild-type kidney image and (B) PKD-affected kidney image.

the ultimate objective of developing a non-invasive technique to monitor disease progression in a PKD mouse model, we performed a preliminary study to investigate the feasibility of using MRI by successfully detailing cyst lesion formation in the jck mouse model. There are clear and marked differences between the MR images of the kidney of PKD mice, relative to those of clinically normal mice. The pattern of dilated tubules generally corresponds to that in histologic slices. The MR images of the enlarged PKD-affected kidneys have high signal intensity tubules, with radial distribution throughout the kidneys, which reflect the dilated collecting ducts associated with infantile PKD.

In clinical applications, renal volume is an important parameter for assessment of patients with kidney disease. Serial kidney volume measurements can be used as an indicator for response to treatment and as a basis for therapeutic decisions. A noninvasive, accurate method for renal assessment that excludes

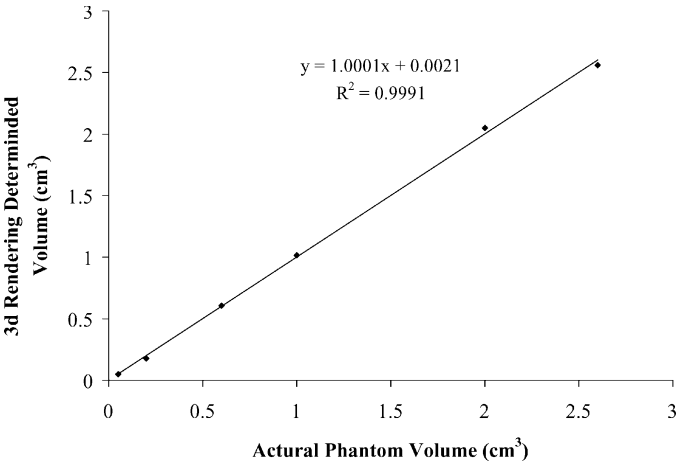

Figure 5. Plot of the actual phantom volume (cm^3) determined using a volumetric pipet versus three-dimensional segmentation-determined volume (cm^3).

ionizing procedures, that can be repeated in the course of the patient's treatment and that follows developmental changes is highly desirable.

Ultrasonography is used for measuring kidney size in most clinical studies. This method is based on the assumption that the kidney resembles an ellipsoid (10, 11). This technique, however, is prone to inaccuracy because it does not take into account the variability in shape of the kidney, and is further hampered by poor repeatability (12, 13). From the results of our in vivo study, using the ellipsoid method on 2-D MRI slices, the renal volume was systematically underestimated by 22% when the transverse renal diameters at the hilum were used for calculating the volumes. We believe the underestimation is due to the fact that the kidney does not represent a true ellipsoid structure.

Volume calculation from 3-D segmented MRI images, using 3-D slicer software, has been validated by us in phantom experiments (Fig. 5) and by others in several organ systems and was found to be accurate (14-17). For example, Fielding and co-workers (14) used a combination of axial MR source images and 3-D models created with 3-D slicer software to describe the anatomy of the normal pelvic floor in young nulliparous women and measured the volume of the levator ani muscle. Dumanli and coworkers (16) used segmentation techniques with a 3-D slicer to determine the volume of the normal female cervix. Using the 3-D segmentation method, the volumes of all voxels within the boundary of the kidney are summed, thus giving the total volume of the kidney. The advantage of this method is that the shape of the kidney is irrelevant and there is reduced risk of obtaining inaccurate volume measurements. Our findings indicate that, for accurate calculation of renal volume, the 3-D MRI segmentation method is preferred over the ellipsoid method using 2-D MRI.

The ability to non-invasively assess cystic disease in mouse models of PKD has a variety of applications. Of considerable importance is the ability to observe progression of this disease without sacrificing the animal, an advantage that will generate a more comprehensive picture of the animal's natural history, compared with the "snapshot" histologic analysis obtained at an arbitrarily determined single time point. This is particularly important for mouse models of PKD, since the rate of disease progression can vary substantially among different models, as well as among different genetic backgrounds (18-20). In fact, the factors that contribute to permutations of this disease are of considerable interest to the research community. Genetic modifiers that affect progression of disease represent alternative targets for therapeutic intervention, and diagnostic tools facilitating their characterization are highly desirable.

An additional application for this non-invasive technology is in concert with a recent renewal in the application of chemical mutagenesis in the mouse. Ethyl-nitrosourea is a potent mutagen, efficiency of which has been well established, and a number of large scale screens have been initiated to develop new mouse models of human disease (21, 22). Non-invasive imaging technology represents an efficient method for surveying mutagenized cohorts for visceral abnormalities.

Magnetic resonance imaging can also be used to study the degree of morphologic change and retardation in mice treated with various drugs. It also saves a considerable amount of expense in animal maintenance and sectioning associated with traditional histologic staining approaches to disease characterization. The jck mouse has a relatively long life span, compared with that of other murine models of PKD, and thus, is a useful model for initiating MRI studies to follow development of this disease. Further studies will concentrate on the tracking of cyst development in the newborn jck mouse, monitoring the volume changes over time, and assessing the effectiveness of various nutritional/pharmacologic therapies for PKD. A further goal is the application of this technique to other mouse models of PKD, such as those carrying targeted mutations of the mouse *PKD1* and *PKD2* genes (23-26).

Acknowledgments

This study was supported by grant NIH S10 RR14792. Dr. Stayner was supported by a New Zealand Foundation for Research, Science and Technology Postdoctoral Fellowship.

Table 1. Kidney volume measurements

Mouse	Kidney	Vh (mm^3)[a] (ellipsoid)	Vm (mm^3)[b] (ellipsoid)	V3d (mm^3)[c] (segmentation)	Comparison[d] (Vh ~ V3d)	Comparison[e] (Vm ~ V3d)
Wild-type (n = 1)						
	Left	135.6	156.9	178.2	-23.9%	-12.0%
	Right	146.9	165.6	187.8	-21.8%	-11.8%
PKD (n = 1)						
	Left	535.2	603.3	690.3	-22.4%	-12.6%
	Right	558.6	608.7	695.1	-19.6%	-12.4%
Average					-21.9%	-12.2

[a,b]Kidney volume measured when the width was determined at the hilum and at the maximal transverse diameter, respectively.
[c]Kidney volume measured, using three-dimensional slicer software.
[d]Comparison = (Vh – V3d)/V3d * 100%.
[e]Comparison = (Vm – V3d)/V3d * 100%

References

1. **Beier, D. R, C. C. Morton, A. Leder, R. Wallace, and P. Leder.** 1989. A mutation caused by integration of a transgene into distal mouse chromosome 15. Genomics **4(4):**498-504.
2. **Atala, A, M. R. Freeman, J. Mandell, and D. R. Beier.** 1993. A new mouse mutation which causes polycistic kidneys. Kidney Int. **43:**1081-1085.
3. **Levine, E. and J. J. Grantham.** 1987. Perinephric hemorrhage in autosomal dominant polycystic kidney: CT and MR findings. J. Comput. Assist. Tomogr. **11:**108-111.
4. **Towner, R. A., T. Yamaguchi, D. J. Philbrick, B. J. Holub, E. G. Janzen, and H. Takahashi.** 1991. In vivo proton magnetic resnance imaging and localized spectroscopic analysis of polycystic kidney disease in DBA/2FG-pcy mice. Magn. Reson. Imaging **9:**429-434.
5. **Hihara, T, H. Ohnishi, O. Muraishi, T. Makil, H. Kumagai, and G. Uchiyama.** 1993. MR image of seminal vesicle cysts associated with adult polycystic kidney disease. Radiat. Medi. **11:**24-26.
6. **Ogborn, M. R., S. Sareen, J. Prychitko, R. Buist, and J. Peeling.** 1997. Altered organic anion and osmolyte content and excretion in rat polycystic kidney disease: an NMR study. Am. J. Physiol. **272:**F63-F69.
7. **Prasad, P. V. and A. Priatna.** 1999. Functional imaging of the kidneys with fast MRI techniques. Eur. J. Radiol. **29:**133-148.
8. **Iakoubova, O. A., H. Dushkin, and D. R. Beier.** 1995. Localization of a murine recessive polycystic kidney disease mutation and modifying loci that affect disease severity. Genomics **26(1):**107-114.
9. **Bakker, J., M. Olree, R. Kaatee, E. E. De Lange, and F. J. A. Beek.** 1997. In vitro measurement of kidney size: comparison of ultrasonography and MRI. Ultrasound Med. Biol. **24:**683-688.
10. **Edell, S. L., A. B. Kurtz, and M. D. Rifkin.** 1990. Normal renal ultrasound measurements, p. 146-160. *In* B. Goldberg, A. Kurtz (ed.), Atlas of ultrasound measurements. Mosby-Year Book Publishers, Chicago.
11. **Bartrum, R. J., E. H. Smith, C. J. D. Orsi, and J. Dantono.** 1974. The ultrasonic determination of renal transplant volume. J. Clin. Ultrasound **2:**281-285.
12. **Ablett, M. J., A. Coulthard, R. E. J. Lee, D. L. Richardson, T. Bellas, J. P. Owen, M. J. Keir, and T. J. Butler.** 1995. How reliable are ultrasound measurements of renal length in adults? Br. J. Radiol. **68:**1087-1089.
13. **Emamian, S. A., M. B. Nielsen, and J. F. Pedersen**. 1995. Intraobserver and interobserver variations in sonographic measurements of kidney size in adult volunteers. A comparison of linear measurements and volumetric estimates. Acta Radiol. **36:**399-401.
14. **Fielding, J. R., H. Dumanli, A. G. Schreyer, O. Shigeo, D. T. Gering, K. H. Zou, R. Kikinis, F. A. Jolesz.** 2000. MR-based three-dimensional modeling of the normal pelvic floor in women. AJR **174:**657-660.
15. **Johnson, L. A., J. D. Pearlman, C. A. Miller, T. I. Young, and K. R. Thulborn.** 1993. MR quantification of cerebral ventricular volume using a semiautomated algorithm. AJNR **14:**1373-1378.
16. **Dumanli, H., J. R. Fielding, D. T. Gering, and R. Kikinis.** 2000. Volume assessment of the normal female cervix with MR imaging: comparison of the segmentation technique and two geometric formulas. Acad. Radiol. **7:**502-505.
17. **Jolesz, F. A., A. Nabavi, and R. Kikinis.** 2001. Integration of interventional MRI with computer-assisted surgery. J. Magn. Reson. Imaging **13:**69-77.
18. **Kuida, S., and D. R. Beier.** 2000. Genetic localization of interacting modifiers affecting severity in a murine model of polycystic kidney disease. Genome Res.**10:**49-54.
19. **Guay-Woodford, L. M., W. J. Green, J. R. Lindsey, and D. R. Beier.** 2000. Germline and somatic loss of function of the mouse cpk gene causes biliary ductal pathology that is genetically modulated. Hum. Mol. Genet. **9:**769-778.
20. **Woo, D. D., D. K. Nguyen, N. Khatibi, and P. Olsen.** 1997. Genetic identification of two major modifier loci of polycystic kidney disease progression in pcy mice. J. Clin. Invest. **100:**1934-1940.
21. **Hrabe de Angelis, M. H., H. Flaswinkel, H. Fuchs, B. Rathkolb, D. Soewarto, S. Marschall, S. Heffner, W. Pargent, K. Wuensch, M. Jung, A. Reis, T. Richter, F. Alessandrini, T. Jakob, E. Fuchs, H. Kolb, E. Kremmer, K. Schaeble, B. Rollinski, A. Roscher, C. Peters, T. Meitinger, T. Strom, T. Steckler, F. Hholsboer, T. Klopstock, F. Gekeler, C. Schindewolf, T. Jung, K. Avraham, H. Behrendt, J. Ring, A. Zimmer, K, K. Schughart, Pfeffer, E. Wolf, and R. Balling.** 2000. Genome-wide, large-scale production of mutant mice by ENU mutagenesis. Nat. Genet. **25:**444-447.
22. **Nolan, P. M., J. Peter, M. Strivens , D. Rogers, J. Hagan, N. Spurr, I. C. Gray, L. Vizor, D. Brooker, E. Whitehill, R. Washbourne, T. Hough, S. Greenaway, M. Hewitt, X. Liu, S. McCormack, K. Pickford, R. Selley, C. Wells, Z. Tymowska-Lalanne, P. Roby, P. Glenister, C. Thornton, C. Thaung, J. A. Stevenson, R. Arkell , P. Mburu, R. Hardisty, A. Kiernan, A. Erven, K. P. Steel, S. Voegeling, J. L. Guenet, C. Nickols, R. Sadri, M. Nasse, A. Isaacs, K. Davies, M. Browne, E. M. Fisher, J. Martin, S. Rastan, S. D. Brown, and J. Hunter.** 2000. A systematic, genome-wide, phenotype-driven mutagenesis programme for gene function studies in the mouse. Nat. Genet. **25:**440-443.
23. **Lu, W, B. Peissel, H. Babakhanlou, A. Pavlova, L. Geng, X. Fan, C. Larson, G. Brent, and J. Zhou.** 1997. Perinatal lethality with kidney and pancreas defects in mice with a targetted *PKD1* mutation. Nat. Genet. **17(2):**179-181.
24. **Lu, W., X. Fan, N. Basora, H. Babakhanlou, H. Babakhanlou, T. Law, N. Rifai, P. C. Harris, A. R. Perez-Atayde, H. G. Rennke, and J. Zhou.** 1999. Late onset of renal and hepatic cysts in *PKD1*-targeted heterozygotes. Nat. Genet. **21(2):**160-161.
25. **Kim, K, I. Drummond, O. Ibraghimov-Beskrovnaya, K. Klinger, M. A. Arnaout.** 2000. Polycystin 1 is required for the structural integrity of blood vessels. Proc. Natl. Acad. Sci. U S A **97(4):**1731-1736.
26. **Wu, G, G. S. Markowitz, L. Li, V. D. D'Agati, S. M. Factor, L. Geng, S. Tibara, J. Tuchman, V. Cai, J. H. Park, J. van. Adelsberg, H Jr. Hou, R. Kucherlapati, W. Edelmann, and S. Somlo.** 2000. Cardiac defects and renal failure in mice with targeted mutations in *PKD2*. Nat. Genet. **24(1):**75-78.